POLITECNICO DI TORINO
Repository ISTITUZIONALE

Assessing the interaction of an energy tunnel with the underground thermal conditions in an urban area

Original
Assessing the interaction of an energy tunnel with the underground thermal conditions in an urban area / Barla, M., Insana, A., Alvi, M.R.. - In: GEOTHERMICS. - ISSN 0375-6505. - ELETTRONICO. - 130:(2025), pp. 1-17. [10.1016/j.geothermics.2025.103350]

Availability:
This version is available at: 11583/2999489 since: 2025-04-24T08:37:09Z

Publisher:
Elsevier

Published
DOI:10.1016/j.geothermics.2025.103350

Terms of use:

This article is made available under terms and conditions as specified in the corresponding bibliographic description in the repository

Publisher copyright

(Article begins on next page)

27 November 2026

Geothermics 130 (2025) 103350



Contents lists available at ScienceDirect

Geothermics

journal homepage: www.elsevier.com/locate/geothermics



Assessing the interaction of an energy tunnel with the underground thermal conditions in an urban area

M. Barla, A. Insana *, M.R. Alvi

Department of Structural, Geotechnical and Building Engineering, Politecnico di Torino, Turin, Italy

ARTICLE INFO

Keywords:
Shallow geothermal systems
Thermo-hydraulic modelling
Thermal interferences
Thermally affected zones
Energy tunnels

ABSTRACT

In the very shallow depths of urban areas it is difficult to find natural undisturbed underground thermal conditions because of anthropic interventions. Moreover, these areas are being increasingly used for energy purposes, for example implementing the technology of shallow geothermal systems to provide clean thermal energy and supply the thermal demand of buildings in both winter and summer seasons. The heat exchanged by these types of renewable energy technologies, in particular ground source heat pump systems such as open loop and closed loop ones, in combination with further anthropogenic activities, results in altered thermal regimes in the subsurface. Energy tunnels, which are achieved by thermally activating the tunnel lining, have recently gained attention among closed loop geothermal systems. Therefore, when planning an urban energy tunnel, attention has to be devoted to the initial underground thermal conditions and to the interactions the pre-existing thermal regime will have with the energy tunnel itself. To this aim, the paper outlines a methodological approach which is then applied to a case study in Turin, Italy, where a new metro line is planned. Thermo-hydraulic numerical modelling is adopted to reproduce the thermally disturbed subsurface environment in the study area prior to the energy tunnel's thermal activation, due to the presence of multiple heat sources (open loop and closed loop systems, underground buildings, car parks and infrastructures), as well as after its commissioning. Results are illustrated in terms of temperature maps and cross sections where the thermally affected zones due to open loop, mainly, and closed loop systems are depicted depending on the operational mode of the shallow geothermal systems. Those results highlight that, when the installation of a new energy tunnel is envisaged, it is necessary to consider the current geothermal exploitation of the area and the operation of neighbouring similar systems.

1. Introduction

Due to the rise of awareness regarding the challenge of climate change and greenhouse gas emissions (GHG), in recent years the European Union has increased its involvement in climate change mitigation policies. Promoted by the booming fossil fuel consumption and excessive GHG, renewable energies have received important backing worldwide through the Paris Agreement signed at the World Climate Summit in 2015. For this reason, investing in renewable energy sources has become a vital and urgent matter. Geothermal energy represents a large source of environmentally friendly energy with a low carbon footprint (Saner et al., 2010) and, thus, shows a high potential to help supplying the thermal demand of buildings in urban areas that are usually characterized by a high-density population. In particular, technologies for the heating-cooling building sector utilizing geothermal heat pumps (GHP) could provide such energy requirements; this technology presented a total installed power of >50 GW in 2015 (Lund and Boyd, 2016) thus, showing a large potential for the mitigation of climate change in this sector (Gaur et al., 2021).

Due to GHP environmental and economic feasibility (Junghans, 2015), a steady increase of their installed capacity worldwide has been observed over the last 20 years. The two main widespread configurations are closed loop and open loop. The former, also called ground source heat pump (GSHP), uses a circuit of pipes embedded in the ground, often within concrete grouting, to exchange heat with the ground. The latter, also called groundwater heat pump (GWHP), takes advantage of groundwater or surface water directly as a heat source and circulates it through heat exchangers placed at the surface, finally discharging it into another well or into the same water reservoir (Edenhofer et al., 2012). Thereby, differently from closed loop geothermal systems, they exchange both heat and mass (i.e. groundwater). GWHP systems are the oldest type of GHP and were the most widely used until the 90s,

* Corresponding author.
E-mail address: alessandra.insana@polito.it (A. Insana).

https://doi.org/10.1016/j.geothermics.2025.103350
Received 17 December 2024; Received in revised form 1 April 2025; Accepted 17 April 2025
0375-6505/© 2025 The Author(s). Published by Elsevier Ltd. This is an open access article under the CC BY-NC-ND license (http://creativecommons.org/licenses/by-nc-nd/4.0/).

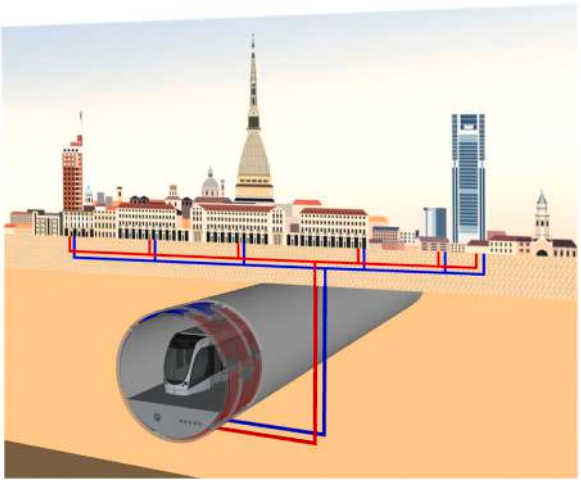

Fig. 1. Energy tunnel concept (out of scale).

when their popularity dropped as increased environmental regulations, designed to prevent aquifer and surface water contamination, have favored the adoption of the GSHPs (Mock et al., 1997). Cold (heating mode) or warm plumes (cooling mode) may develop during the operations of the geothermal plant, inducing thermal alterations in the ground. It is conventionally accepted to name 'Thermally Affected Zone (TAZ)' the area that experiences a temperature variation higher than 1 K (Di Dato et al., 2022; Lo Russo et al., 2014; Barla et al., 2018). TAZs represent a potential anthropogenic source of pollution that needs to be considered during the design of the system to avoid interferences with existing groundwater applications and underground infrastructure, particularly in densely populated urban areas. The concern about the development of the abovementioned thermal anomalies is growing worldwide as they may cause considerable wasting of the heat exchange potential (Epting and Huggenberger, 2013) and failures of geothermal energy plants (Herbert et al., 2013). Despite this, open loop schemes are still commonly used in several countries and urban areas since their large technical potential for heating and cooling buildings is state of fact.

Compared to open loop, in closed loop systems there is a reduced risk of environmental damage during operation; hence, they can potentially be installed in almost every site and, in addition, there is no particular technical restriction which prevents their installation. An innovative type of closed loop system is represented by energy geo-structures. They can be defined as all those ground-contact structures that provide both structural support and an energy contribution to the climatization of buildings. Piles, micropiles, diaphragm walls, anchors and, the most recently investigated, tunnel linings can be mentioned among this technology (Laloui and Di Donna, 2013; Barla and Perino, 2015; Barla et al., 2019). Energy tunnels take advantage of the large volume for heat exchange granted by the, usually, long longitudinal extension of the underground infrastructures (e.g. metro lines in urban environment, Insana and Barla, 2020; Barla and Insana, 2023). The thermal activation is achieved by embedding a network of absorber pipes in the structural elements inside which a fluid circulates to exchange heat with the surrounding ground (Fig. 1). Differently to the previously mentioned technologies (GWHP, GSHP, energy piles) which are generally local installations, energy tunnels peculiarity lies in the fact that the thermally activated structure will interact with a wider area of the urban environment, potentially leading to interferences with or being affected from existing installations.

Researchers have provided comprehensive studies focusing on potential thermal interferences between shallow geothermal systems (SGS) where the presence of groundwater flow contributes to the formation and the migration of thermal plumes (Alcaraz et al., 2016; Alcaraz and Vives, 2017). The continuously growing use of subsurface resources in urban areas for energy purposes may lead to conflicting uses or overexploitation and depletion (Ferguson and Woodbury, 2006; Quattrocchi et al., 2013; Vienken et al., 2015; García-Gil et al., 2020; Epting et al., 2020). In this context, interactions among different geothermal users and with other subsurface uses are becoming more and more frequent and may result in strong alteration of the available geothermal potential (Fry, 2009; Herbert et al., 2013; Barla et al., 2018; Baralis and Barla, 2024). To the best knowledge of the authors, only few researchers have addressed the thermal interactions with energy geostructures, especially in urban densely populated areas. Therefore, insights into the potential interactions between SGS in an urbanized area are of utmost relevance and will be investigated in this paper.

As a fundamental step for an energy tunnel design, the assessment of its interaction with the ground and other users is to be studied. In this paper a methodological procedure is outlined to explore such

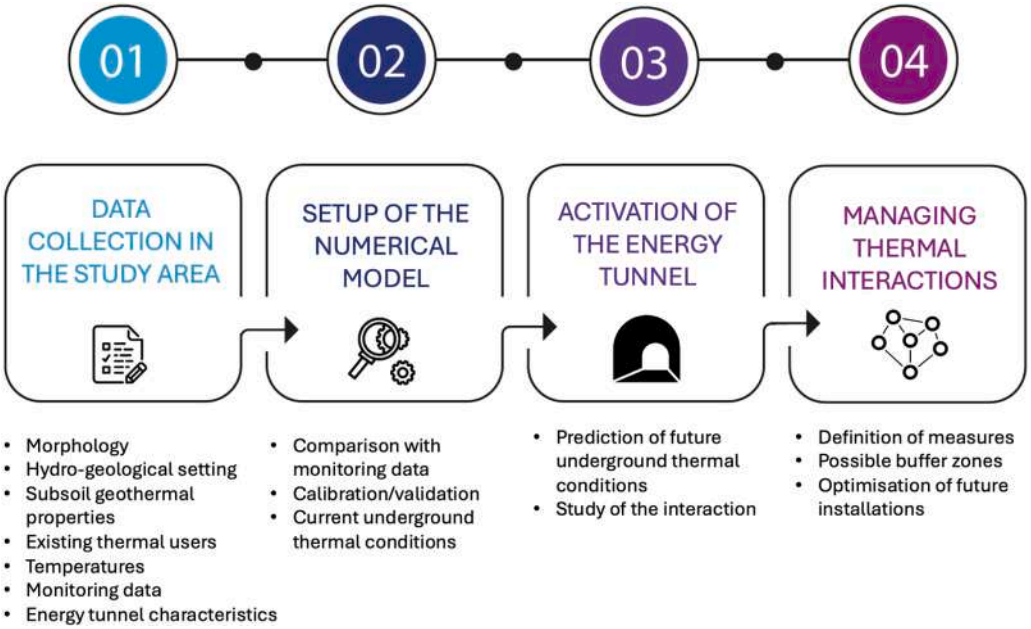

Fig. 2. Methodological process for the assessment of the interaction of the energy tunnel with the existing users in an urban environment.

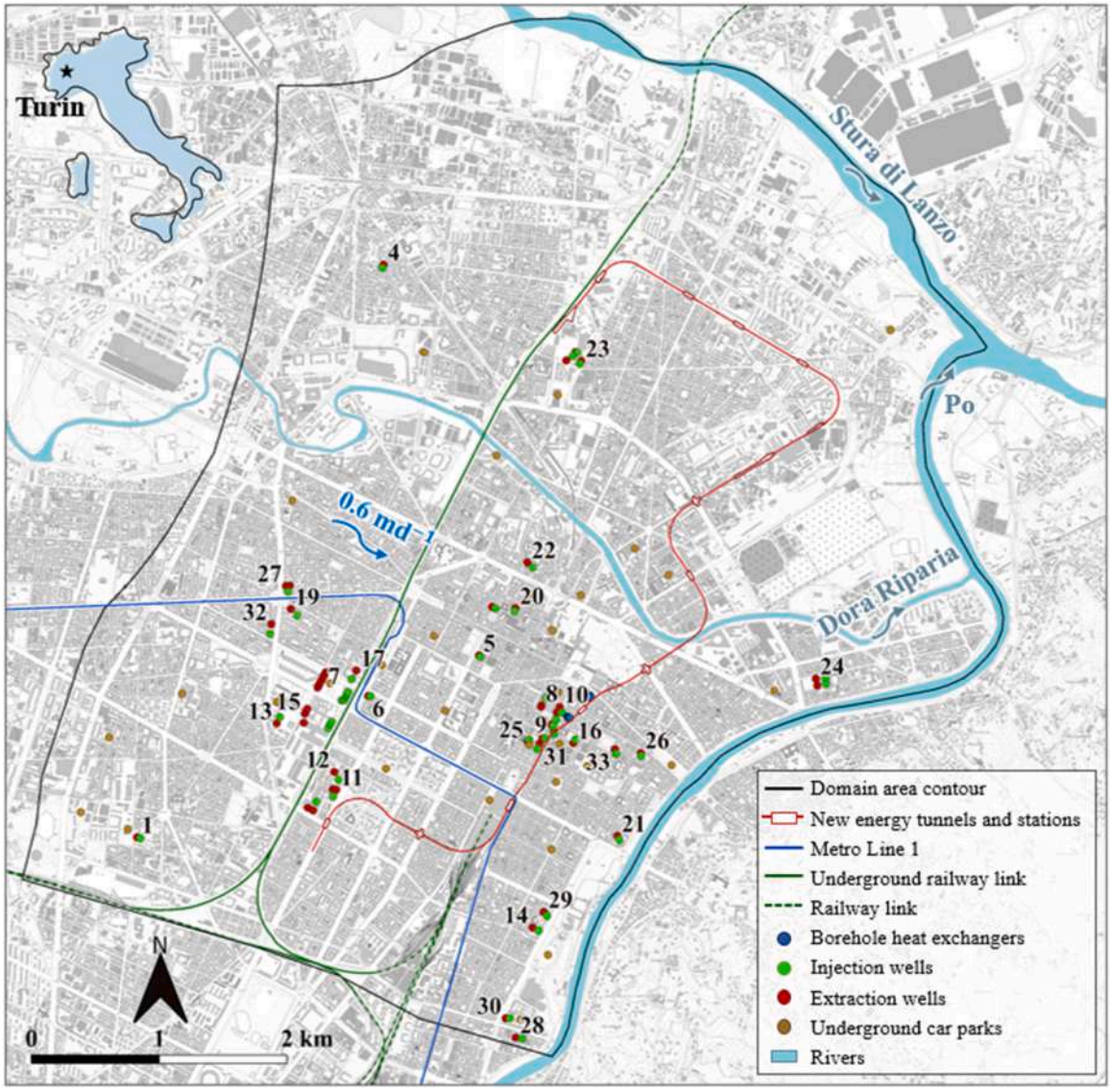

Fig. 3. Map of the study area with the indication of the new energy metro line and the existing main users impacting the shallow thermal environment.

interaction. Then, reference will be made to the case of Turin's central districts, where a new metro line with thermally activated lining is planned. Finite Element thermo-hydraulic modelling will be adopted to reproduce the current thermal environment of the subsoil, simulating the operation of the current installations present. Then, the same model will consider the thermal activation of the geostructure to assess the interaction with the existing installations.

2. The energy tunnel in an urban area

When a thermally activated metro tunnel is planned in an urban area, the issue arises to study its interaction with the pre-existing installations and users of the ground heat. Any metro line, in fact, will typically cross the city for many kilometers, encountering other infrastructures and/or man-made activities. When urban tunnels are designed to be thermally active and are supposed to exchange heat with the surrounding ground, depending on the actual usage of the underground, positive or negative thermal interactions with pre-existing activities may occur in some specific locations. As an example, if the metro tunnel crosses an area where open loop geothermal systems are active, the heat exchange of the energy tunnel lining may be reduced because of the interception with the thermal plume of the existing geothermal systems. Conversely, the tunnel itself may impact the potential exploitation of shallow geothermal systems if they are located in the area which is affected by the heat exchange between the ground and the tunnel.

Because of the above, within the design process of an energy tunnel, a specific effort should be devoted to study the thermo-hydraulic behaviour of the tunnel in the real environment. To this extent three-dimensional Finite Element thermo-hydro coupled numerical models are of great help.

With the purpose of assessing the interaction between the energy tunnel and the existing users, a four steps methodological process is outlined in Fig. 2. The first step requires the collection of all the information for the selected study area. This includes the morphology, hydrogeology and geothermal properties of the subsoil, data on existing ground heat users such as shallow geothermal open and closed loop systems, buildings basements, underground car parks, etc. and, of course, the characteristics of the energy tunnel. Ground and/or groundwater temperatures monitoring data must be collected together with the operational data from the active systems. A thermo-hydro coupled numerical model is then built to reproduce the relevant area. First, calibration of key parameters takes place to tune some of the model's parameters and reproduce the monitored data in a certain

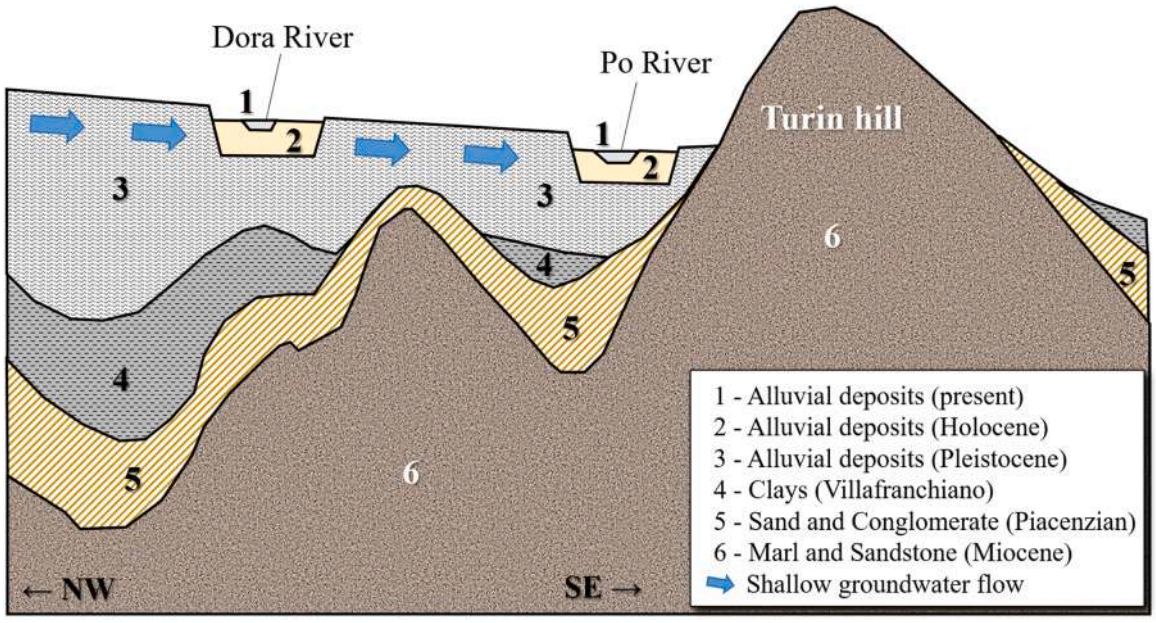

Fig. 4. Representative schematic (out of scale) geological section of Turin city area (modified from Bottino and Civita, 1986).

timeframe. Then, the model is validated against the collected monitoring data in a different timeframe. Once a reliable model is established, able to fully reproduce the actual behaviour of the subsoil thermal environment as affected by the existing users, the activation of the energy tunnel is to be simulated to evaluate its interaction with the existing users. On the basis of the results obtained from the model and with reference to a defined time frame, specific measures may be evaluated and defined to minimise interaction and/or optimise the location of future installations.

In the following the above methodological process will be exemplified with reference to the case of a metro line to be constructed in the city of Turin (Italy), where pre-existing thermal harnessing of the subsoil has been taking place since many years by open and closed loop geothermal systems as well as by industrial activities.

3. Data collection

An overview of the study area, that includes the central districts of Turin (Italy) where a new metro line is going to be constructed in the coming years, is depicted in Fig. 3.

From a morphological point of view, the area of interest is located in the narrow portion of the western Po plain in northwestern Italy, enclosed by the rivers Stura di Lanzo, Sangone and Po, with elevation that varies between 210 and 270 m a.s.l. The river Po serves as the major drainage for the watershed and flows northeast along the western border of the Turin hill.

The geological setting of the plain area is rather well-known thanks to numerous borehole drilling (Regione Piemonte, 2007) and the experience gained with multiple deep foundations and urban tunnel projects (Barla and Barla, 2005; 2012). The geological stratigraphy includes (see Fig. 4):

- Coarse alluvial fluvioglacial deposits (corresponding to units 1–3 in Fig. 4), mainly constituted by pebbles, gravel, and sand in a sandy-silty matrix; this layer represents the upper 25–50 m of Turin subsoil. The thickness decreases moving from the southern to the northern part of the urban area. Its heterogeneity is accentuated due to the highly variable degree of cementation. Cemented portions are distributed randomly and originate lenses with the characteristics of conglomerate rock, also known by the term Puddinga.
- Villafranchiano formation (corresponding to unit 4 in Fig. 4), a succession of lacustrine and fluvial-lacustrine deposits represented by clays and silts locally including gravel lenses whose origin is the Middle Pliocene - Lower Pleistocene.
- Ancient terrigenous succession of sand deposits and fossiliferous conglomerates (unit 5 in Fig. 4) and marl alternating sandstone (unit 6 in Fig. 4) originated in the Miocene - Middle Pliocene (Piacenzian).

As mentioned, cemented soil is often present in the fluvioglacial deposits due to calcareous deposition processes. Direct observation in the field has indeed shown that cemented areas of ground are generally randomly distributed along horizontal layers, with thickness varying between a few centimetres to a few meters (Barla and Camusso, 2008). This heterogeneity was properly taken into account at the district macro scale thanks to maps retrieved from the literature where the cementation degree statistically occurs between 0–25 %, 25–50 % and 50–75 % (de Rienzo and Oreste, 2011), identified as C1, C2 and C3. However, these maps did not cover the entire study area; for this reason, they were extended based on recent data collected from hydrogeological and geognostic campaign surveys. The geothermal properties pertaining to the zones C1, C2 and C3 were also assessed on the basis of field tests carried out in the area of interest (Barla et al., 2013).

The shallower geotechnical unit hosts an aquifer whose thickness ranges from 15 to 30 m and is underlined by the thick Villafranchiano clayey formation where the aquitard is located. The main direction of the unconfined aquifer's flow, that extends over the entire urban plain (including the study area), is from North-West to South-East towards the Po river (Civita and Pizzo, 2001).

Thanks to the presence of the very productive shallow aquifer and to easy access to water (maximum depth of the water table approximately 20–25 m), the studied area has been experiencing extreme interest in shallow geothermal energy. In fact, an exponential growth in the number of open loop systems was documented (Lo Russo et al., 2014; Barla et al., 2018). A specific survey carried out by the Authors in the Metropolitan City of Turin's repository highlighted, at the time of writing, the presence of 34 open loop systems (for a total of 109 extraction and re-injection wells). Thanks to this survey, it was possible to know the position of each well and piezometer belonging to the various open loop systems together with their monitoring data (temperature, pump rates and hydraulic heads) and their bottom depths

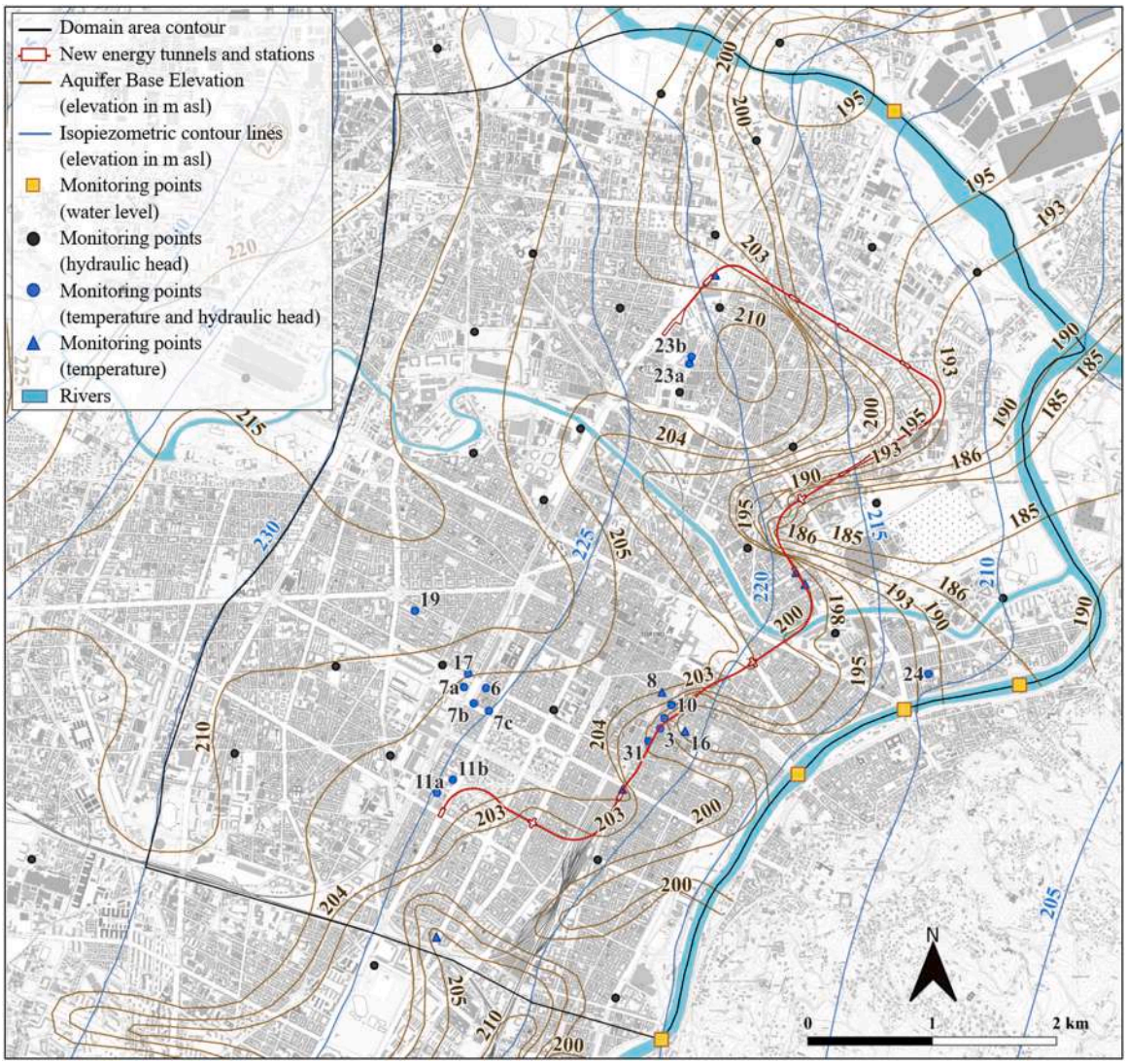

Fig. 5. Map of the aquifer data collected in the study area.

(ranging from 21 to 49 m). The distance between the extraction and re-injection wells of the plant varies from 17 to 215 m and the mean wells diameter is 35.5 cm. The characteristics of two closed loop systems (having 5 and 7 geothermal probes, respectively, 113 m depth and total installed power of 6 kW) within the study area are also known and were considered as well. These existing shallow geothermal installations (open and closed loop systems), which can be listed among the so-called active users because they exchange mass and/or heat with the aquifer and directly exploit the shallow geothermal resource, are shown in Fig. 3 (in which monitoring points were excluded for the sake of clarity).

The same figure also highlights the new thermally activated metro line and stations, whose path is indicated in red, together with the other anthropic structures, like the Metro Line 1, railway link and underground car parks. Given the purpose of this study, not only the track but also other characteristics of the new energy tunnel must be collected, like the depths interested by the infrastructure, its geometry and the excavation methods. In this case, the energy tunnels will be excavated partly with the Cut&Cover technique, partly with a Tunnel Boring Machine. In the first case, pipes are embedded in the diaphragm walls while for the TBM tunnels, the heat exchanger circuits are fixed to the steel cage before casting of the concrete segments. The depth of the energy tunnel and stations is not constant along the route: the Cut&Cover tunnels reach an average depth of 10 m, while the TBM tunnels reach greater depths, up to a maximum of 34 m below the ground surface and with an average equal to 25 m. The TBM tunnel external diameter is 9.60 m. The maximum depth of the underground stations' diaphragm walls, instead, is 32 m.

With the exception of the new energy tunnel, these anthropic entities, as well as the buildings' underground levels (that are not shown in the Figure for the sake of clarity), can be classified as passive users, since they still impact the underground thermo-hydraulic environment by exchanging heat fluxes with the subsurface because of their underground location.

All the relevant information was collected in a Geographic Information System (GIS) environment. The GIS dataset built includes the topography (Digital Terrain Model, DTM), the base aquifer elevation data, the groundwater surface elevation, the location of the piezometers inside and on the boundaries of the domain, the open and closed loop

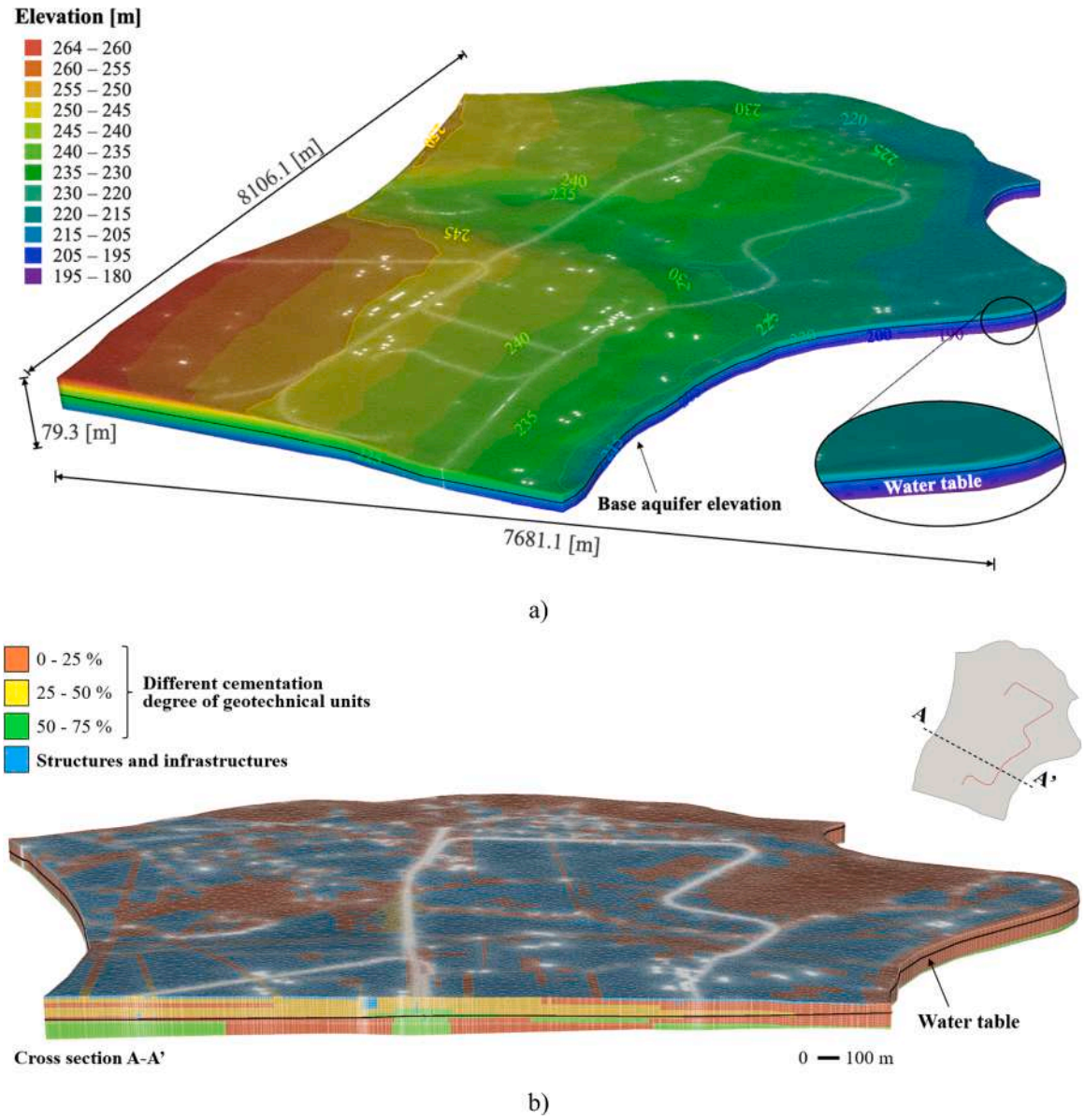

Fig. 6. 3D numerical model: (a) dimensions and elevation; (b) section showing the distribution of the different degree of cementation within the geotechnical units.

systems, the track of the existing underground infrastructures (railway link, Metro Line 1), the footprint of the underground levels of buildings and car parks and, finally, the path of the new energy tunnel envisaged.

Fig. 5 illustrates the aquifer base elevation, isopiezometric contour lines and the available monitoring points. Specifically, the monitoring data of the rivers' water levels and of the piezometers' hydraulic heads (indicated in Fig. 4 with yellow squares and with black points respectively) were collected from direct measurements and from the metropolitan authority monitoring network (ARPA Piemonte). This dataset was used as model input (as described in Chapter 4). Instead, hydraulic heads and temperature data collected in the monitoring points indicated in blue in Fig. 5 (blue squares and triangles) were collected in the framework of the urban energy tunnel's design and utilized to validate the model output. The groundwater surface elevation and isopiezometric contour lines, together with the shallow aquifer baselines, allowed to properly assess the top and base elevation of the unconfined groundwater body. With other information provided by the monitoring network, a satisfying knowledge of the unconfined aquifer conditions was finally achieved.

The Western boundary of the study area (and, therefore, of the numerical model that will be later described) was chosen to match one isopiezometric contour line, while the Eastern boundary coincides with the Po river. The Southern and part of the Northern boundaries were chosen perpendicular to the isopiezometric contour lines, while the remaining part of the Northern boundary coincides with the Stura di Lanzo river.

4. Set-up of the numerical model

On the basis of the information collected, a three-dimensional Finite Element numerical model was built by using the commercial code FEFLOW (DHI, 2022). Thanks to the interoperability features between

Table 1
Material hydraulic and thermal properties adopted in the numerical model.

Materials	Property	Symbol	Unit	Value
Coarse alluvial fluvioglacial deposits: geotechnical unit C1 (cementation degree 0–25 %)	Horizontal hydraulic conductivity	$K_x = K_y$	ms^{-1}	$(0.4–3.9)\cdot10^{-3}$
	Vertical hydraulic conductivity	K_z	ms^{-1}	$(0.2–1.98)\cdot10^{-4}$
	Specific storage	S	m^{-1}	10^{-4}
	Porosity	n	–	0.175
	Anisotropy ratio	–	–	0.05
	Solid thermal conductivity	λ_s	$Wm^{-1}K^{-1}$	4.19
	Solid volumetric thermal capacity	$\rho_s c_s$	$MJm^{-3}K^{-1}$	1.8
	Longitudinal dispersivity	α_L	m	3.1
	Transverse dispersivity	α_T	m	0.31
Coarse alluvial fluvioglacial deposits: geotechnical unit C2 (cementation degree 25–50 %)	Horizontal hydraulic conductivity	$K_x = K_y$	ms^{-1}	$(0.45 - 2.8)\cdot10^{-3}$
	Vertical hydraulic conductivity	K_z	ms^{-1}	$(0.22–1.46)\cdot10^{-4}$
	Specific storage	S	m^{-1}	10^{-4}
	Porosity	n	–	0.15
	Anisotropy ratio	–	–	0.05
	Solid thermal conductivity	λ_s	$Wm^{-1}K^{-1}$	3.75
	Solid volumetric thermal capacity	$\rho_s c_s$	$MJm^{-3}K^{-1}$	1.7
	Longitudinal dispersivity	α_L	m	3.1
	Transverse dispersivity	α_T	m	0.31
Coarse alluvial fluvioglacial deposits: geotechnical unit C3 (cementation degree 50–75 %)	Horizontal hydraulic conductivity	$K_x = K_y$	ms^{-1}	$(0.4–2.3)\ 10^{-3}$
	Vertical hydraulic conductivity	K_z	ms^{-1}	$(0.21–1.2)\cdot10^{-4}$
	Specific storage	S	m^{-1}	10^{-4}
	Porosity	n	–	0.125
	Anisotropy ratio	–	–	0.05
	Solid thermal conductivity	λ_s	$Wm^{-1}K^{-1}$	3.3
	Solid volumetric thermal capacity	$\rho_s c_s$	$MJm^{-3}K^{-1}$	1.7
	Longitudinal dispersivity	α_L	m	3.1
	Transverse dispersivity	α_T	m	0.31
Concrete	Horizontal hydraulic conductivity	$K_x = K_y$	ms^{-1}	10^{-16}
	Vertical hydraulic conductivity	K_z	ms^{-1}	10^{-16}
	Specific storage	S	m^{-1}	10^{-4}
	Porosity	n	–	0
	Anisotropy ratio	–	–	1
	Solid thermal conductivity	λ_s	$Wm^{-1}K^{-1}$	1.12
	Solid volumetric thermal capacity	$\rho_s c_s$	$MJm^{-3}K^{-1}$	2.19

the geo-referred database and the numerical code, the entities in the model were geo-referred and the mesh generator was forced to comply with their geometrical constraints. A Triangle mesh generator (Shewchuk, 1996) was adopted to partition the model domain in 355600 elements per layer, with 178232 nodes per slice (5334000 elements and 2851712 nodes in total). The 3D model's plan dimensions are 8106 m x 7681 m (Fig. 6a). The bottom boundary of the model corresponds to the base aquifer elevation. The domain encompasses the alluvial deposits shown in Fig. 4.

Three geotechnical units, all within the alluvial deposits, with a different degree of cementation (C1, C2, C3) were considered as defined in the work of de Rienzo and Oreste (2011). Thanks to the interoperability between the GIS environment and the software, the maps showing the distribution of the three geotechnical units in the study area were introduced to define the spatial distribution of C1, C2 and C3 in the model (Fig. 6b). The hydraulic and thermal properties of the geotechnical units used as input are provided in Table 1. These units were considered orthotropic from a hydraulic point of view, according to the origin of the deposit. The anisotropy is correlated with the sedimentary genetic processes of the soils which determine in most cases a more or less evident stratification of the materials that generally corresponds to a greater degree of permeability to horizontal motions compared to vertical ones; the deposition process, indeed, induces vertical hydraulic conductivities 10 to 20 times smaller than the horizontal values. The calibration of the hydraulic conductivity of the geotechnical units was obtained thanks to an optimization process with PEST utilities (Doherty and Hunt, 2010) and the results of pumping tests performed in a central portion of the modelled area in previous studies (Barla et al., 2013; Baralis, 2015; 2016; Baralis, 2020; Baralis and Barla, 2024).

Soil thermal dispersivity (with the typical ratio between transverse and longitudinal values equal to 1/10) was derived from calibrations obtained in previous studies for the same site (Barla et al., 2013). The assessment of this property is indeed very difficult and could be managed through *in situ* tests, like tracer tests (Epting and Huggenberger, 2013), which, however, are accompanied by uncertainties related to the problem scale effects (Sethi and Di Molfetta, 2007). Given also the difficulties coming with direct determination of properties such as porosity and heat capacity, using values from literature was considered more reasonable (Celico, 1988; VDI 4640 2001; Eppelbaum et al. 2014). The thermal conductivity of the geotechnical units was obtained from *in situ* tests, i.e. Thermal Response Tests, carried out at different locations in the Turin metropolitan area for the geostructure's thermal design purposes (Insana et al., 2023).

Finally, underground anthropic structures (namely tunnels, car parks and building basements) were assigned concrete material properties and were considered with isotropic characteristics from the hydraulic point of view, as indicated in Table 1. Moreover, depths pertaining to buildings and car parks were assessed considering their relevant number of underground storeys; specifically, one underground level buildings were considered up to 2.5 m, two underground levels buildings up to 7.5 m and those with three or more underground levels according to their actual depths.

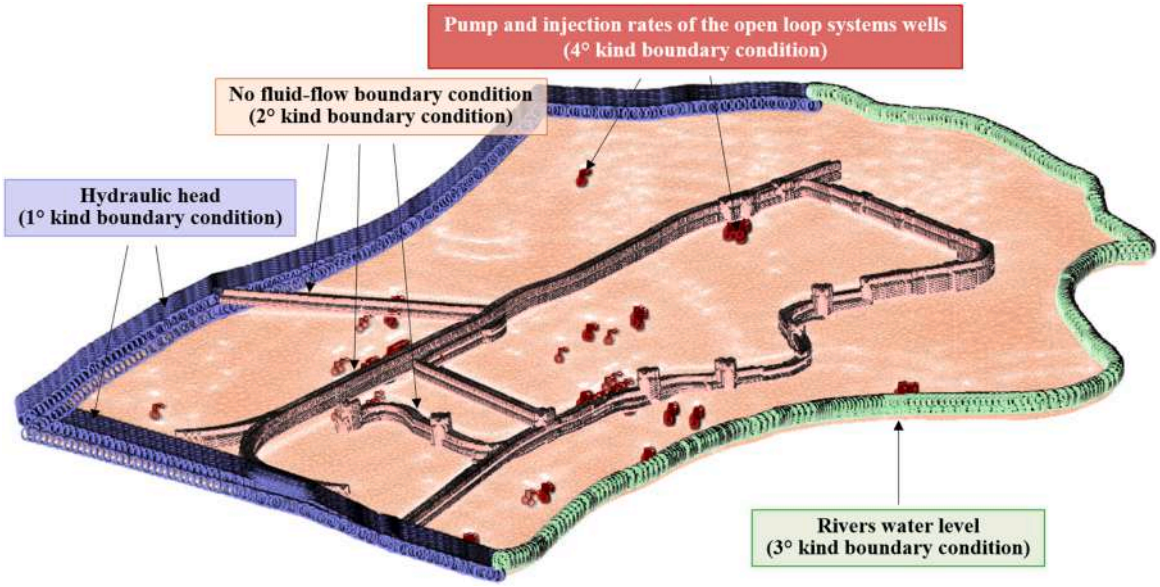

Fig. 7. Hydraulic boundary conditions of the coupled thermo-hydraulic numerical model.

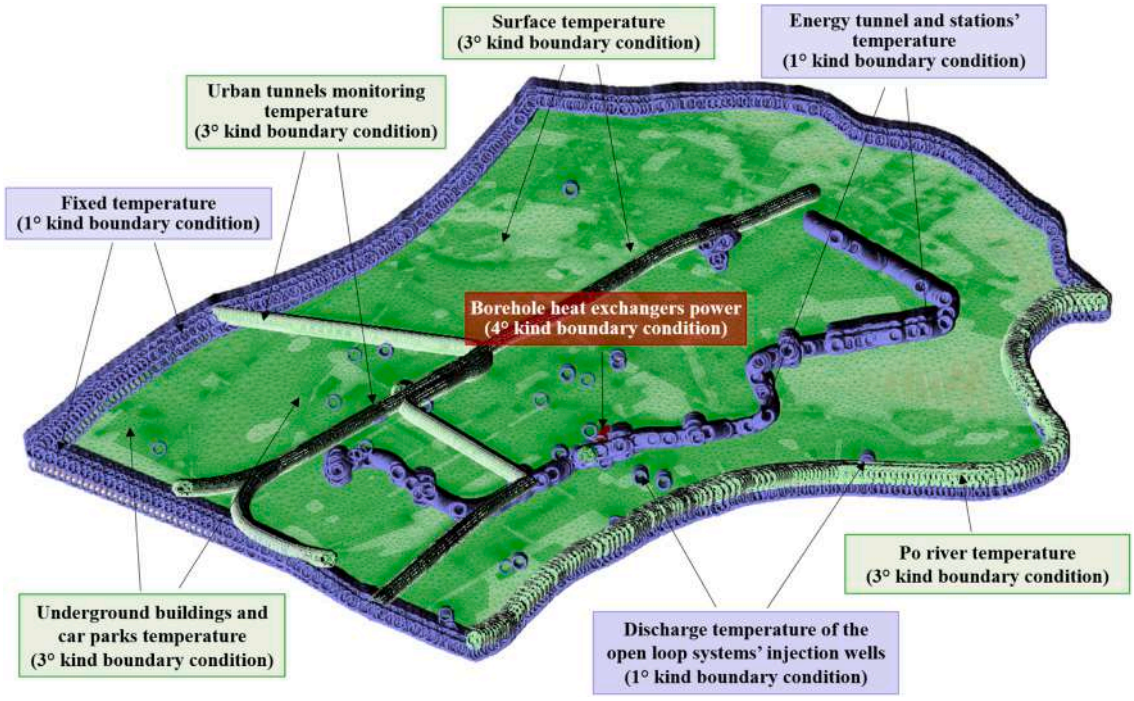

Fig. 8. Thermal boundary conditions of the coupled thermo-hydraulic numerical model.

4.1. Hydraulic boundary and initial conditions

The mean piezometric surface was extrapolated from the monitoring data and was set as the initial hydraulic head throughout the domain. The initial water table depth varies throughout the domain: in the North-Eastern portion it is at its minimum (4 m below the ground surface), while in the South-Western portion it reaches the maximum depth of 27.5 m (indicated in Fig. 6 with the black line).

To define the hydraulic boundary conditions (Fig. 7), data histories retrieved from water level monitoring points (indicated with the yellow squares in Fig. 4) and piezometers closer to the external borders of the study area (shown with black points in Fig. 4) were automatically interpolated (or extrapolated) along the boundaries of the numerical model adopting a 1st kind boundary condition (Dirichlet-type). Such boundary condition is typically imposed along boundaries on which seepage can occur, where groundwater level is well-known. In the case of the boundaries corresponding to the Po and the Stura di Lanzo rivers, the measured water level was imposed as 3rd kind boundary condition

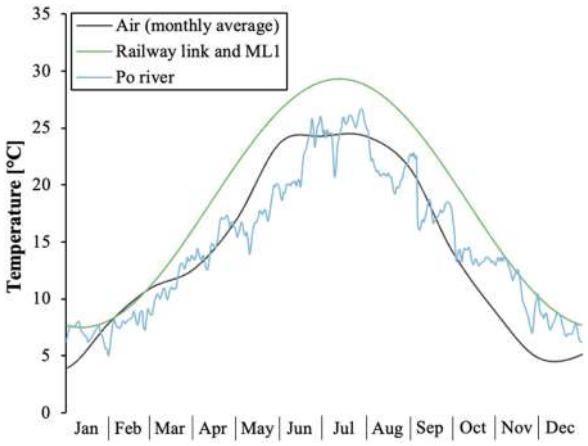

Fig. 9. Air, railway link and Metro Line 1, and Po river temperature profile imposed as boundary condition.

(Cauchy-type, with the transfer rate of 650 d^{-1}), suitable for surface water bodies (Diersch, 2014).

For the anthropic structures in the aquifer (i.e. urban tunnels and underground stations) a no fluid-flux boundary condition (2nd kind BC) was imposed since they are impermeable.

Finally, to simulate the open loop systems, a sink/source internal boundary condition (4th kind BC) was set to the mesh nodes included in the screening interval of each extraction and injection well (with proper sign values). The pumping and injection rates time histories associated with each open loop system were assigned based on monitoring data, when available. Alternatively, authorized limits given by the local authority were assigned.

4.2. Thermal boundary and initial conditions

The temperature of 14.5 °C was initially set throughout the domain and fixed at the North, West, South and part of the East boundaries' nodes as a 1st kind boundary condition (as shown in Fig. 8), which is commonly adopted where the temperature is known or predefined at

Table 2
Thermal transfer data adopted for the thermal sources/sinks.

Natural or anthropic entities	Property	Symbol	Unit	Value
Open surface (air)	Heat transfer rate	h_c	$Wm^{-2}K^{-1}$	0.145
	Temperature	T	°C	2.9 – 26
Po river	Heat transfer rate	h_c	$Wm^{-2}K^{-1}$	0.015
	Temperature	T	°C	5.0 – 26.6
Underground levels of buildings	Heat transfer rate	h_c	$Wm^{-2}K^{-1}$	0.3
	Temperature	T	°C	17
Underground car parks	Heat transfer rate	h_c	$Wm^{-2}K^{-1}$	0.3
	Temperature	T	°C	17
Urban tunnels	Heat transfer rate	h_c	$Wm^{-2}K^{-1}$	2.19
	Temperature	T	°C	7.5 – 29.3

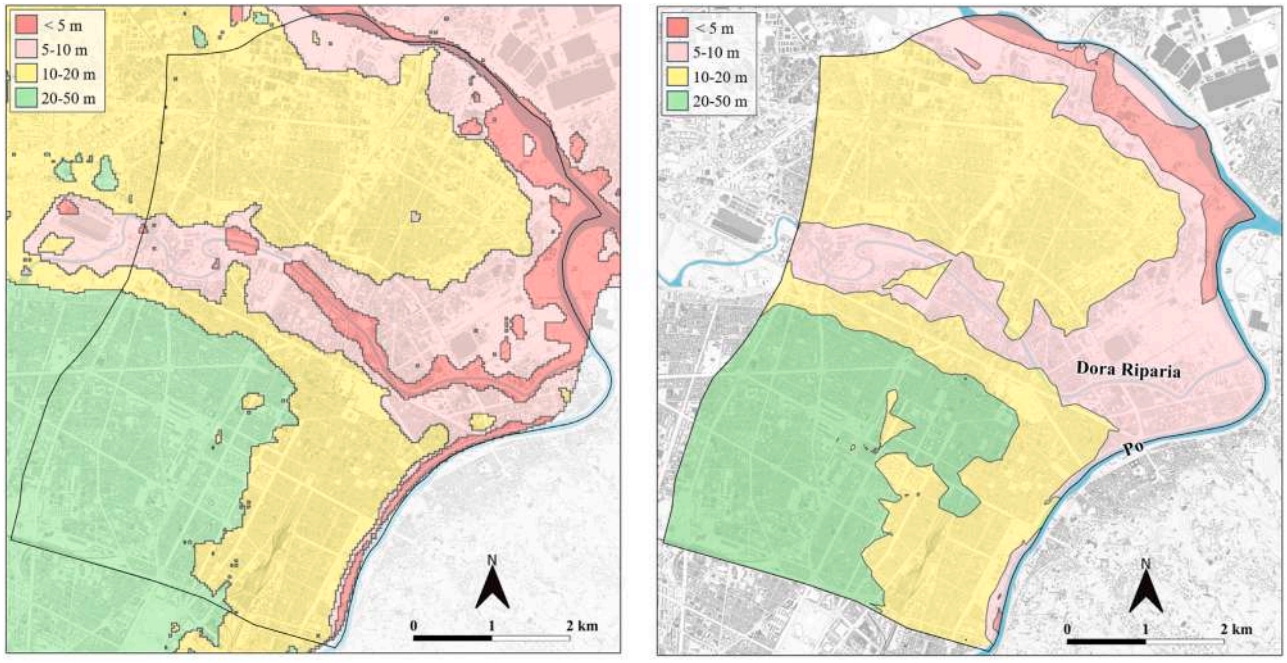

Fig. 10. Water table depth in the model area: (a) interpolation of measurements from the Geoportale of the Piedmont regional authority (ARPA Piemonte, 2020) and (b) calculated values by numerical analysis.

inflow or outflow boundaries (Diersch, 2014). This value was selected according to the temperatures monitored through piezometers located inside and in the surroundings of the domain since their recorded value was considered representative of the underground undisturbed thermal conditions. On the remaining upper part of the East boundary the recorded values of Po river temperature during the year 2021 (Fig. 9, data are similar in other years as well) was applied as a 3rd kind boundary condition. The heat transfer rate was selected according to Epting and Huggenberger (2013). In the 3rd kind thermal boundary condition a fixed/transient reference temperature is imposed with a heat transmission coefficient (i.e. heat transfer rate) and is applied in cases where the reference temperature is linked to the temperature of groundwater via a separating heat-conductive medium. As stated by Diersch (2014), this specific boundary condition is commonly used to simulate the heat transfer through river boundaries, and air-contact surfaces (e.g. tunnels and underground buildings).

The average monthly air temperature computed from the year 2021 measured daily values (Fig. 9) was applied as a 3rd kind boundary condition to the area of the uppermost slice of the model where no buildings or other structures are present. The influence of the solar radiation contribution was considered negligible for the aim of this study, given the depths influenced by the energy tunnels, underground stations and the other shallow geothermal systems present in the modelled area and was neglected as in similar studies (Epting and Huggenberger, 2013; Herbert et al., 2013; Perego et al., 2022; Baralis and Barla, 2024).

The operation of the many open-loop systems in the area was reproduced by applying the recorded injection temperature time series (1st kind boundary condition) to the nodes reproducing the injection wells of each geothermal plant. It is noted that the existing systems are activated in the model at the time corresponding to their installation.

The closed-loop systems (i.e. borehole heat exchangers) were introduced as nodal sink/source boundary conditions (4th kind BC). Since the only available information on the energy performance of the closed-loop system was the total installed power, the thermal power demanded to the ground was calculated hypothesizing an average geothermal heat pump Coefficient of Performance (COP) of 4. The heat extraction/injection rate to the ground was then divided by the number of nodes containing heat sink/source BCs from the first layer to the last one (Perego et al., 2022).

Underground levels of buildings, underground car parks and urban tunnels (with the exception of the new energy tunnel that will be introduced in the thermal activation phase) were associated with the temperatures and heat transfer rate values listed in Table 2 (3rd kind BC). On one hand, the constant temperature of 17 °C assumed for all the underground levels was derived from monitoring data reported by Tinti et al. (2015). On the other hand, the urban tunnels temperature profile (Fig. 9) was assumed by sinusoidal approximation of measured values recorded in Turin Metro Line 1 (Barla et al., 2016).

The heat transfer rates imposed on the open surface (pertaining to air) and to the Po river are the same as in Epting et al. (2013) and Baralis (2020). Those selected for buildings and underground car parks refer to the minimum required by law (Ministero dello Sviluppo Economico, 2015) for climate zone E in which Turin is located. Urban tunnels' heat transfer rate h_c, instead, was estimated for simplicity considering the average thickness of the concrete lining s equal to 30 cm, the thermal conductivity of concrete λ_s and the air heat transfer rate $h_{c,air}$ of 5.3 $Wm^{-2}K^{-1}$ (Insana and Barla, 2020; Insana, 2020):

$$h_c \left[Wm^{-2}K^{-1}\right] = \left[h_{c,air}^{-1} + \frac{s}{\lambda_s}\right]^{-1} \quad (1)$$

To simulate the thermal activation of the new energy metro line, pertinent temperature boundary conditions (1st kind) were fixed on the mesh nodes corresponding to the tunnel and diaphragm walls extrados and to the stations' underground walls in contact with the ground. Overall, almost 200 different temperature values were considered, depending not only on the position of tunnel lining and diaphragm walls with respect to groundwater flow, but also on the season (Barla et al., 2021). These values are not constant through the tunnel's path but vary according to the thermal design of the infrastructure. For the Cut&Cover tunnels, the working temperature applied ranged between 7.1 and 9.4 °C and 22 and 24.4 °C for the winter and summer seasons respectively. For the TBM tunnels, the assessed working temperature ranged between 6.4 and 10.8 °C and 21.1 and 25.8 °C for the winter and summer seasons respectively. The operating temperature imposed to the underground stations' diaphragm walls were between 7.7 to 14.4 °C in winter and 19.7 and 24.6 °C in summer.

4.3. Validation of the existing thermal environment

The validation phase had the purpose of reproducing the current thermo-hydraulic environment in the subsoil, prior to the thermal activation of the energy geostructure. After having set up the model, the first numerical analysis was performed by simulating a timeframe of 5 years (2017–2021), where the only active geothermal energy systems were the open loop ones and the borehole heat exchangers.

The accuracy of the calculated water table depth was checked at the end of the 5 years' calculation period by comparing the results with the data available at the Geoportale of Piedmont from ARPA Piemonte (2020). Fig. 10 shows a good agreement between the computed water table depth at the end of the validation phase (Fig. 10b) and the water table depth available on the Geoportale (Fig. 10a). In most of the domain, in those areas where the water table depth is located below 10 m, numerical and reported data are in agreement. A moderate overestimation of the computed values can be found in restricted zones close to the Dora Riparia and Po rivers with the computed values slightly exceeding the range reported by the regional authority of 5 m. However, considering that the energy tunnel, in these areas, is generally located deeper than the calculated water table (as it will be discussed in the next chapter) the mentioned discrepancy will not affect the results.

To further test the consistency of numerical results with respect to real hydro-thermal regime, numerical results were also compared with hydraulic heads and temperatures monitoring data (the location of the monitoring points are indicated with blue points and triangles in Fig. 5) collected from piezometers located downstream the open loop systems' wells in the area (Fig. 11). On one hand, the differences between temperature monitoring data and numerical results did not exceed one degree in most cases; on the other hand, numerical hydraulic heads were slightly lower with respect to monitoring data, consistently with the results related to the water table depth (Fig. 10). Specifically, cross-validation returned a Root Mean Square Error (RMSE) and Mean Absolute Error (MAE) between 0.49 and 1.96 °C for temperature and between 0.1 and 3.5 m for the hydraulic head. RMSE and MAE computed for each of the five monitoring points are summarized in Table 3.

Finally, thermal maps for the winter and summer seasons (2021) are shown in Fig. 12. These maps are useful to show the extension and persistence of the thermal plumes due to the shallow geothermal systems active in the area and the other anthropic activities. The maps shown were obtained through spatial interpolation of numerical results in QGIS and correspond to a depth of 25 m, within the saturated ground. The groundwater flow drives the thermal plumes towards the South-East and the Po river. The central districts of the city, where the largest number of existing geothermal systems are present, are the most influenced area from a thermal perspective. Considering that the new energy tunnel will cross this area, it is envisaged that the thermal plumes of the existing open loop systems could locally affect the thermal exploitation. This aspect will be discussed in the next chapter.

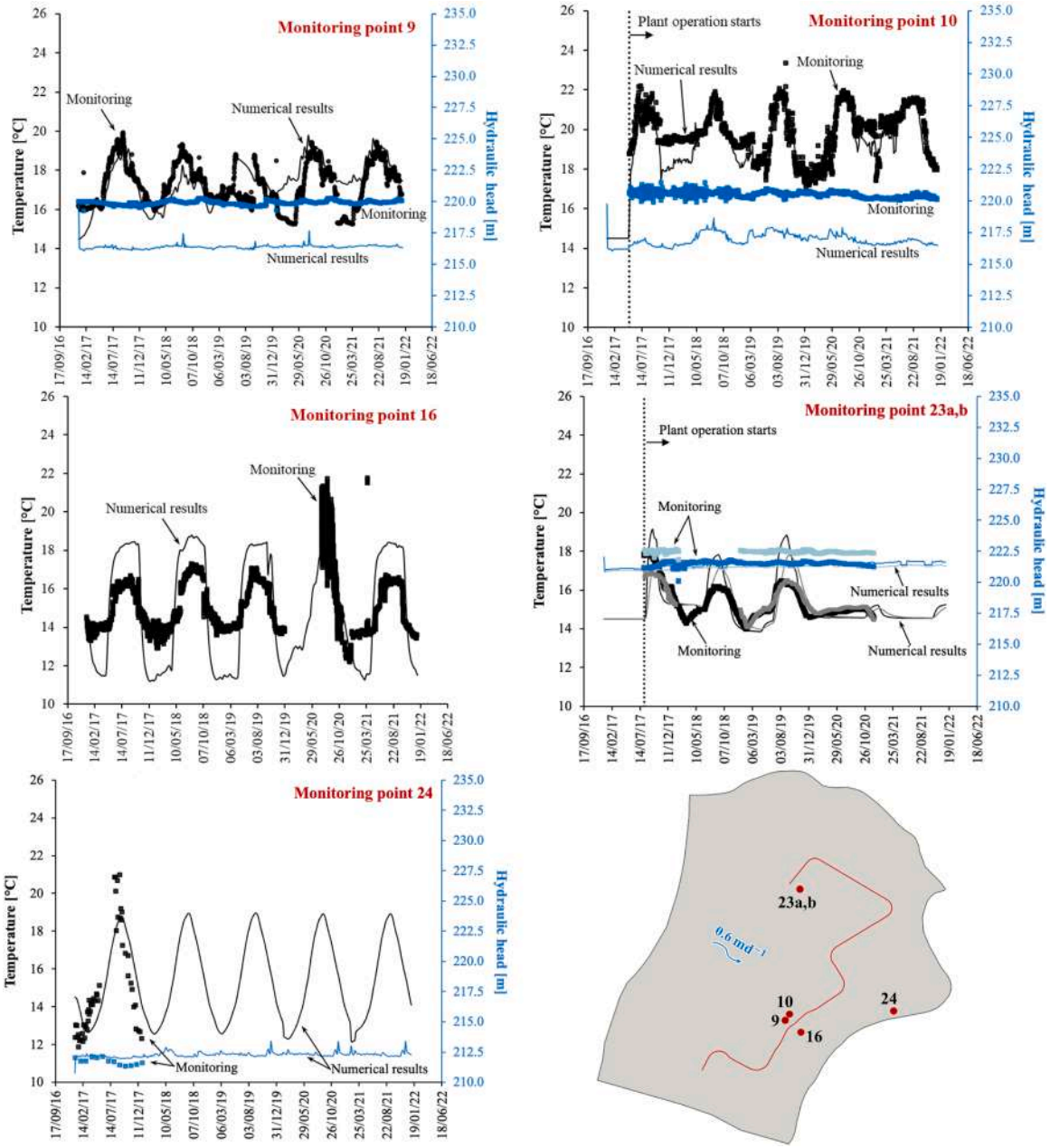

Fig. 11. Comparison among calculated and monitored temperature and hydraulic heads at five different geothermal water wells piezometers.

Table 3
RMSE and MAE for the comparisons of the numerical and monitored data of the five different geothermal water wells piezometers.

	Temperature		Hydraulic head	
	RMSE [°C]	MAE [°C]	RMSE [m]	MAE [m]
Monitoring point 9	1.03	0.82	3.50	3.49
Monitoring point 10	0.68	0.49	3.57	3.54
Monitoring point 16	1.96	1.79	–	–
Monitoring point 23a	0.95	0.71	0.20	0.16
Monitoring point 23b	0.65	0.50	1.30	1.29
Monitoring point 24	1.59	1.38	0.54	0.45

5. Interaction with the new energy tunnel

The numerical analysis described in the previous section allowed the definition of the current representative hydraulic and thermal regimes of the study area. This section will illustrate the interaction between the new energy tunnel, the ground and other users as obtained by the subsequent numerical analysis. In the design process of an energy tunnel, it is indeed of interest to investigate the impact of the existing shallow geothermal users on the energy production of the tunnel as well as the impact of the thermal activation of the tunnel lining on infrastructures and/or systems located nearby.

The thermal activation of the energy tunnels and underground stations, i.e. the heat exchange between the energy geostructures and the surrounding ground, was simulated over a 4-years timespan during which the heating and cooling seasons were cyclically repeated. The heating season was assumed to start on October 15th and to end on April 15th (182 days), while the cooling season was assumed to start on June 1st and to end on August 31st (91 days). During resting periods, the energy geostructures were considered thermally inactive. The open loop systems and borehole heat exchangers were assumed to continue the same level of utilization of the last annual cycle simulated.

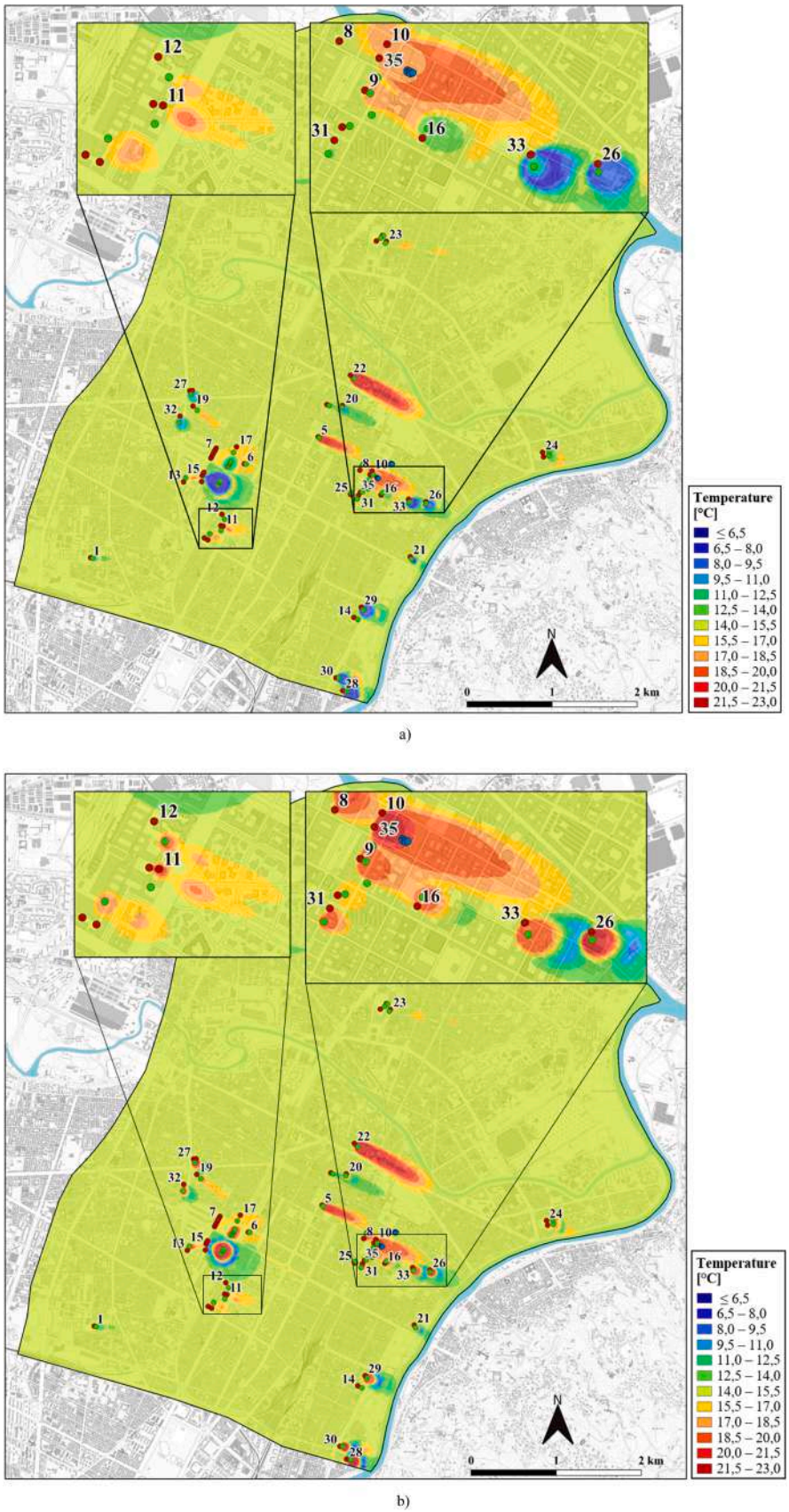

Fig. 12. Thermal maps at the end of (a) winter and (b) summer season 25 m below the ground surface.

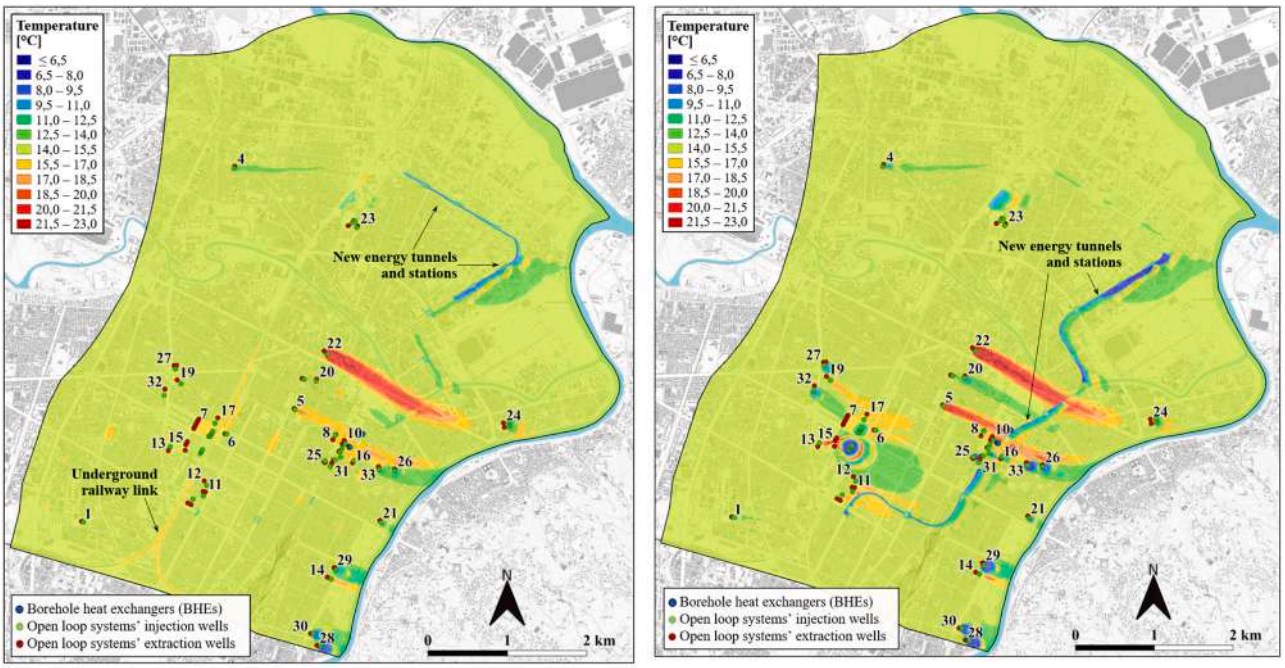

Fig. 13. Thermal maps at the end of the last winter season at a depth of (a) 10 m and (b) 25 m.

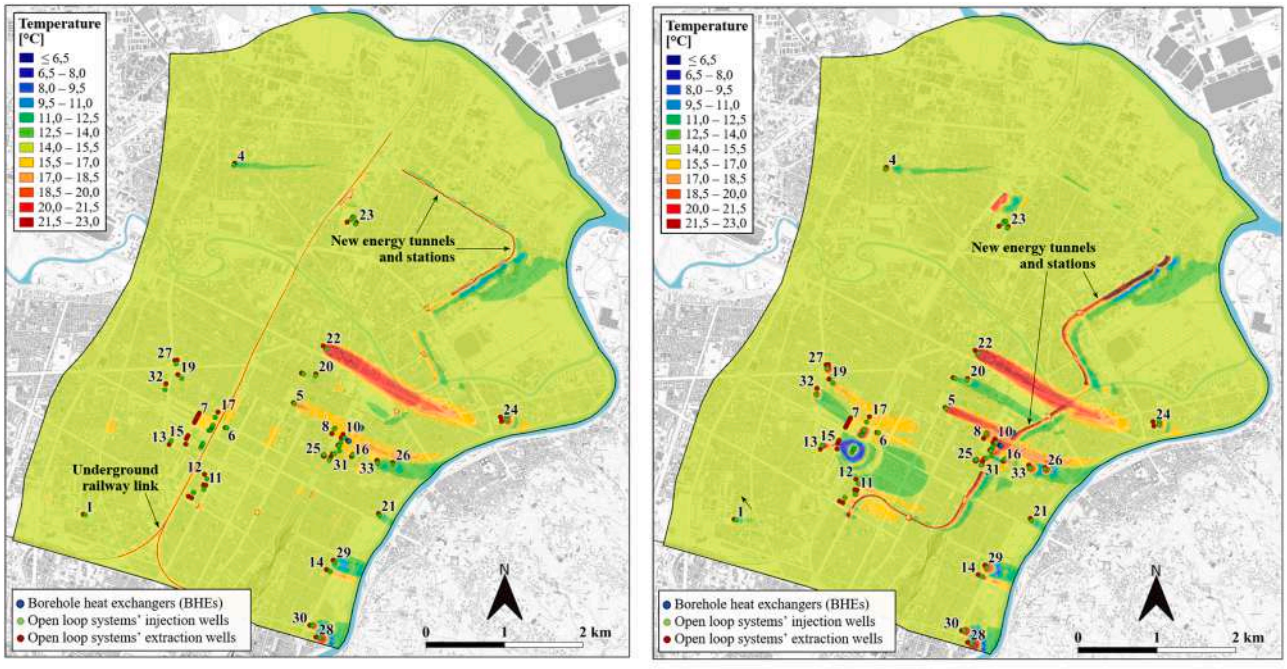

Fig. 14. Thermal maps at the end of the last summer season at a depth of (a) 10 m and (b) 25 m.

Similarly to what was done at the end of the validation phase, thermal maps were obtained at the end of the last simulated winter and summer seasons at the depths of 10 m and 25 m, which correspond to the two main depths of the energy tunnel in the area (Cut&Cover and TBM tunnel sections, respectively). The thermal maps obtained are shown in Fig. 13 (at the end of winter, 15th of April) and in Fig. 14 (at the end of summer, 1st of September).

The result shows that the thermal alteration due to the new energy tunnels and stations is limited to the corresponding depths of the structures and downstream the infrastructure, according to the groundwater flow direction. The most extended areas are located where the groundwater flow direction is perpendicular to the tunnel axis. Also, it is evident that the TAZs surrounding the energy tunnel and metro stations are limited in comparison to those pertaining to open loop geothermal systems. Indeed, the TAZs pertaining to the operation of the open loops are more extended both in winter and summer. This aspect is

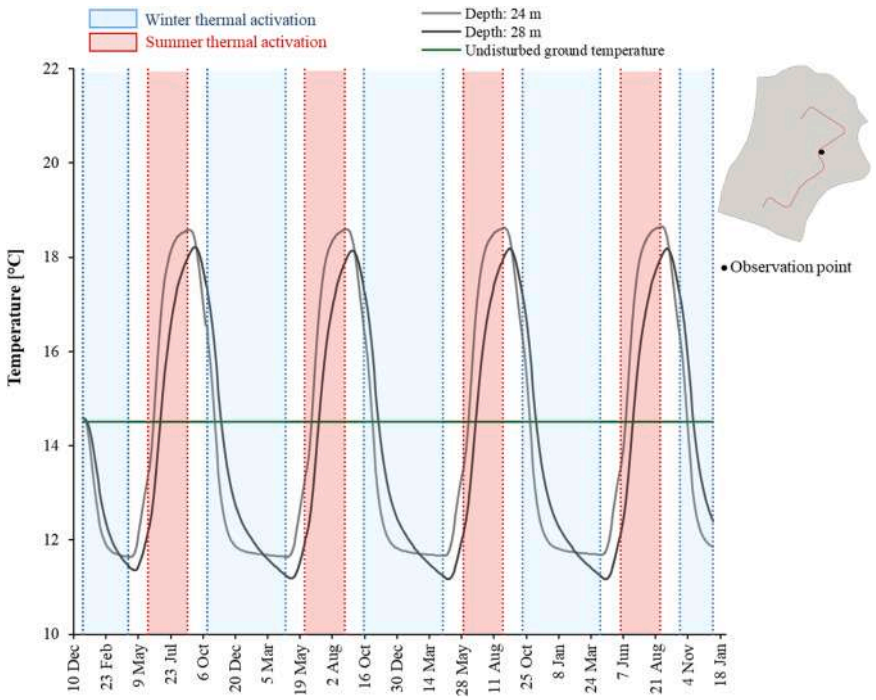

Fig. 15. Undisturbed ground temperature and calculated temperature downstream the energy tunnel.

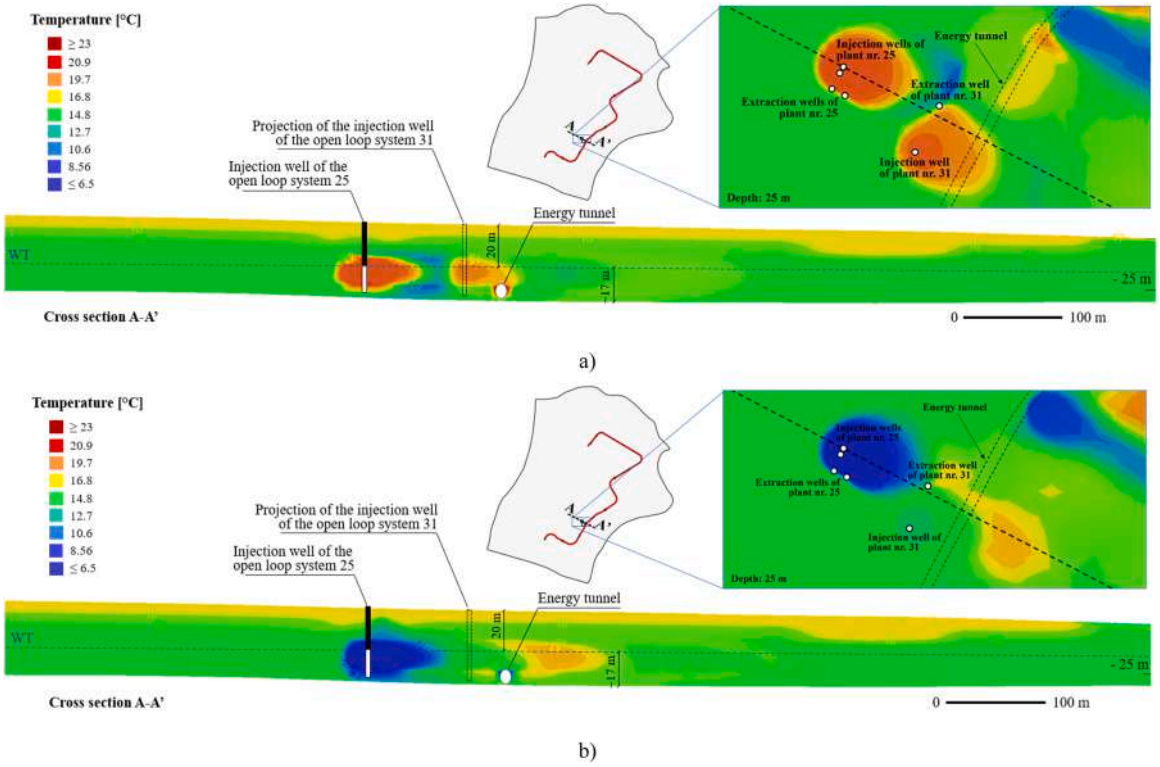

Fig. 16. Cross section A-A': temperature halfway through the last (a) summer and (b) winter season in the activation phase. The scale on the vertical axis has been increased by a factor of 2. WT = Water table.

also confirmed by the comparison of the respective thermal plumes in the 3D sections of the model which will be shown in the following paragraphs. Thereby, as expected, the impact of the energy tunnel to the aquifer can be considered negligible compared to the impact given by the operation of open loop systems since the energy geostructure exchanges only heat and not mass with the underground. Additionally, Fig. 15 illustrates the temperature computed in the numerical model downstream the energy tunnel at 21 m distance (between 2 and 3 times the tunnel diameter) at two depths of interest for the energy tunnel's thermal activation and the undisturbed ground temperature (i.e. before the energy tunnel thermal activation). Numerical results denote the absence of any thermal drift, meaning with this an alteration in

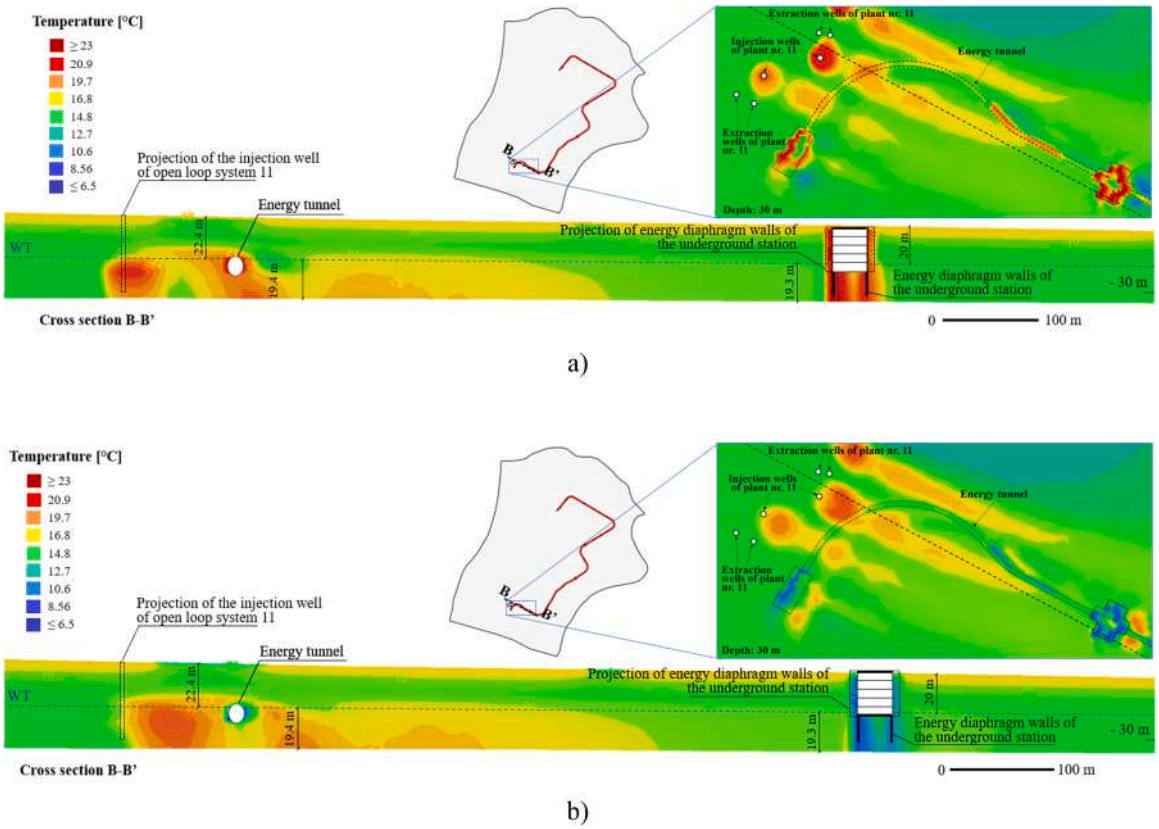

Fig. 17. Cross section B-B': temperature halfway through the last a) summer and b) winter season in the activation phase. The scale on the vertical axis has been increased by a factor of 2. WT = Water table.

underground temperature in the long term due to the operation of the energy tunnel, in areas where only the energy tunnel is present (i.e. without any other operating shallow geothermal energy systems).

In Fig. 16, the impact of the open loop plants nr. 25 and 31 on the energy tunnel is shown halfway through the last summer (Fig. 16a) and winter season (Fig. 16b). For the sake of clarity, the vertical black line refers to the well casing, while the well screen has been shown in white. The water table is indicated with the dashed blue line.

During the cooling season (in summer), the injection well of plant nr. 25 introduces warm water (temperature around 20 °C) in the aquifer, thus originating a thermal plume driven by the groundwater flow in the direction of the energy tunnel (Fig. 16a), which is located downstream and below the groundwater table. However, between plant nr. 25 and the energy tunnel there is also another geothermal installation (that is plant nr. 31, located approximately 85 m far from plant nr. 25) whose thermal plume is also driven by the groundwater flow towards the energy tunnel. The plume generated by the injection well of this latter plant (whose projection is depicted in Fig. 16a) mostly affects the energy tunnel's performance in a negative way during the cooling season, since the injection well of this plant is closer to the infrastructure than the injection well of plant nr. 25. In fact, during summer, the energy tunnel exchanges heat with the ground warming the surrounding aquifer (like the open loop plants) to supply the buildings or stations' cooling loads linked to the energy tunnel circuit. Since the operation of plant nr. 25, primarily, and of plant nr. 31, secondarily increases the temperature of the subsoil and groundwater surrounding the energy tunnel's lining, the efficiency of the energy geostructures will be inevitably affected.

During the heating season (Fig. 16b), the interaction between the open loop plant nr. 25 and the energy tunnel is less evident, since the effect of the former is mitigated by the operation of the open loop plant nr. 31. The latter, in fact, is located between open loop plant nr. 25 and the energy tunnel and injects water at a temperature of 13 °C during the heating season, much warmer with respect to the injection temperature of the open loop plant nr. 25, which is around 7 °C.

Another relevant example of thermal interaction between the energy tunnel and the open loop systems can be found at the South end of the metro tunnel track, where thermal interferences occur with the open loop plant nr. 11 (Fig. 17). This open loop plant operates in cooling mode only, injecting warm water in summer. While this condition is favourable for the heat exploitation by the energy tunnel during the heating season (Fig. 17b), it influences its performance during the cooling summer season (Fig. 17a). Additionally, it can be noticed that the thermal activation of the urban energy geostructure mitigates the thermally altered areas.

In Fig. 17 it can also be seen how the thermal activation of the energy diaphragm walls belonging to one underground station affects the surrounding. As already discussed, the impact of the energy tunnels and stations on the underground thermal environment is limited with the respect to the impact of the other open loop systems operating in the study area. As shown in Fig. 17a, the water table depth can be found at 22.4 m below the ground surface, slightly below the tunnel crown extrados. Like the previous case, thus, the energy tunnel lies in saturated ground. However, the thermal plumes of the energy tunnel and underground station's diaphragm walls (considering the portions below the water table) are less extended of those pertaining to the operation of the injection well of the open loop system 11. As expected, compared to the unsaturated portions of the subsoil directly in contact with the underground station's diaphragm walls (which has a thickness of 20 m as indicated in Fig. 17), longer thermal plumes can be found in the saturated layer, according to the groundwater flow regime. Of course, this also depends on the hydro-thermal properties of the underground (like the thermal conductivity, heat capacity, hydraulic conductivity and the groundwater flow velocity).

6. Conclusions

The growing interest in shallow geothermal resources leads to dense installation areas where the sustainability of the installed systems can be potentially compromised by the insurgence of thermal interferences. This condition must be avoided in those cases where a loss of the performance of these systems could occur. This aspect becomes particularly relevant when an energy tunnel is to be constructed in an already deeply exploited area. Therefore, the assessment of the interaction between the energy tunnel, the ground and other users become a fundamental step in an energy tunnel design process.

In this paper reference was made to the case of Turin's central districts, where a new metro line with thermally activated lining is planned. Finite Element Thermo-Hydraulic modelling was adopted to reproduce the current thermal environment of the subsoil, simulating the operation of the installations currently present. Then, the same model, successfully validated against monitoring data, was used to simulate the thermal activation of the geostructure and assess the interaction with the existing installations.

The integrated use of GIS and numerical analyses was useful to analyse the results obtained. These have shown that the impact of the energy tunnel is restricted to the depths of the infrastructure and bare a limited extension with respect to the thermally altered zones originating by the open loop systems; thereby its impact on the aquifer is considered negligible compared to open loop systems. Additionally, it was observed that the presence of active open loop systems in the area, upstream the energy tunnel, may impact, either positively or negatively, the heat exchange between the latter and the subsoil. Depending on the operating mode (and injection temperature) of the open loop system, in fact, the temperature of the aquifer and subsoil upstream the energy tunnel, before and during the thermal activation of the geostructure, could differ from the undisturbed value, influencing the energy tunnel performance. While positive impact corresponds to a cost-free advantage, improving the payback time of the investment, a negative impact may be detrimental. Anticipating such conditions is indeed crucial at the design stage on one side to avoid overestimation of the geothermal potential, on the other because it allows to put in place timely countermeasures, such as mitigation of the open loop operativity and/or optimisation of the thermally activated sections. The present study enhances the importance of considering the current geothermal use of an urban area when designing new SGS in order not to hinder their future energy exploitation and optimise their use.

CRediT authorship contribution statement

M. Barla: Writing – review & editing, Supervision, Resources, Methodology, Investigation, Funding acquisition, Conceptualization. **A. Insana:** Writing – review & editing, Supervision, Methodology, Investigation, Formal analysis, Data curation, Conceptualization. **M.R. Alvi:** Writing – review & editing, Writing – original draft, Visualization, Validation, Investigation, Formal analysis, Data curation.

Declaration of competing interest

The authors declare that they have no known competing financial interests or personal relationships that could have appeared to influence the work reported in this paper.

Acknowledgments

The project was carried out in the framework of the partnership between Politecnico di Torino and Infra.TO Srl Torino. The Authors would like to acknowledge the Metropolitan City of Turin and Geosolving Srl, Torino, for providing some of the input data.

Data availability

Data will be made available on request.

References

Alcaraz, M., Vives, L., 2017. The T-I-G ER method: a graphical alternative to support the design and management of shallow geothermal energy exploitations at the metropolitan scale. Renew. Energy 109, 213–221. https://doi.org/10.1016/j.renene.2017.03.022.

Alcaraz, M., García-Gil, A., Vázquez-Suñé, E., Velasco, V., 2016. Advection and dispersion heat transport mechanisms in the quantification of shallow geothermal resources and associated environmental impacts. Sci. Total. Environ. 543, 536–546. https://doi.org/10.1016/j.scitotenv.2015.11.022.

ARPA Piemonte, 2020. Idrogeologia (revised 15/12/2020). http://www.arpa.piemonte.it/(accessed 5 November 2023).

Baralis, M., Barla, M., 2024. rOGER: a method for determining the geothermal potential in urban areas. Geothermics 124, 103148. https://doi.org/10.1016/j.geothermics.2024.103148.

Baralis, M., 2015. Studio Delle Condizioni Geotermiche Alla Scala Urbana Della Città di Torino. Master Thesis (in italian), Politecnico di Torino, Turin.

Baralis, M., 2020. Optimisation of Geothermal Resources in Urban Areas. PhD Thesis, Politecnico di Torino, Turin.

Barla, G., Barla, M., 2005. Assessing design parameters for tunnelling in a cemented granular soil by continuum and discontinuum modelling. In: Proceedings of the 11th IACMAG Conference. Turin, pp. 475–484.

Barla, M., Barla, G., 2012. Torino subsoil characterization by combining site investigations and numerical modelling. Geomech. Tunnel. 5 (3), 214–231. https://doi.10.1002/geot.201200008.

Barla, M., Camusso, M., 2008. Using particle elements to model the Torino subsoil mechanical behaviour to improve the applicability of microtunnelling technique. In: Proceedings of the 12th IACMAG Conference, Goa, India,1-6 October 2008, pp. 4299–4305.

Barla, M., Insana, A., 2023. Energy tunnels as an opportunity for sustainable development of urban areas. Tunnel. Undergr. Space Technol. 132, 104902. https://doi.org/10.1016/j.tust.2022.104902.

Barla, M., Perino, A., 2015. Energy from geo-structures: a topic of growing interest. Environ. Geotech. 2 (1), 3–7. https://doi.org/10.1680/envgeo.13.00106. ISSN 2051-803X.

Barla, G., Antolini, F., Barla, M., Bonini, M., Debernardi, D., Perino, A., 2013. Analisi e Verifica Delle Condizioni Di Esercizio in Sicurezza Del Palazzo uffici Provinciali Di Corso Inghilterra 7 Tenuto Conto Del Centro Direzionale Di Intesa Sanpaolo – Modellazione numerica, Analisi Di Interazione e Piano Di Monitoraggio. Technical report (in italian), Politecnico di Torino, Turin.

Barla, M., Di Donna, A., Perino, A., 2016. Application of energy tunnels to an urban environment. Geothermics 61, 104–113. https://doi.org/10.1016/j.geothermics.2016.01.014.

Barla, M., Di Donna, A., Baralis, M., 2018. City-scale analysis of subsoil thermal conditions due to geothermal exploitation. Environ. Geotech. 7 (4), 1–11. https://doi.org/10.1680/jenge.17.00087.

Barla, M., Di Donna, A., Insana, A., 2019. A novel real-scale experimental prototype of energy tunnel. Tunnel. Undergr. Space Technol. 87, 1–14. https://doi.org/10.1016/j.tust.2019.01.024.

Barla, M., Baralis, M., Insana, A.,F., Aiassa, S., Antolini, F., Vigna, F., Azzarone, F., Marchetti, P., 2021. On the thermal activation of Turin Metro line 2 tunnels. Proceedings of International Conference of the International Association For Computer Methods and Advances in Geomechanics, LNCE 126. Springer, Cham, Switzerland, pp. 1069–1076. https://doi.org/10.1007/978-3-030-64518-2_127.

Bottino G., Civita M.V., 1986. Engineering geological features and mapping of subsurface in the metropolitan area of Turin, North Italy. In: 5th International IAEG congress, Buenos Aires, pp. 1741–1753.

Celico P. (1986). Prospezioni idrogeologiche. Vol I, II. Liguori Editore, Napoli (in italian). ISBN: 9788820713317 and 9788820715601.

Civita, M., Pizzo, S., 2001. L'evoluzione spazio-temporale del livello piezometrico dell'acquifero libero nel sottosuolo di Torino. GEAM 38 (4), 271–287 (in italian).

de Rienzo, F., Oreste, P., 2011. Analyses of the distribution and nature of the natural cementation of quaternary sediments: the case of the Turin subsoil (Italy). Geotech. Geol. Eng. 29 (3), 319–328 (Dordr). https://doi.10.1007/s10706-010-9378-5.

DHI, 2022. Finite Element Simulation System For Subsurface Flow and Transport Processes FEFLOW 7.5 (version 7.5) [software]. DHI-WASY GmbH, Berlin.

Di Dato, M., D'Angelo, C., Casasso, A., Zarlenga, A., 2022. The impact of porous medium heterogeneity on the thermal feedback of open-loop shallow geothermal systems. J. Hydrol. 604, 127205. https://doi.org/10.1016/j.jhydrol.2021.127205.

Diersch, H.J.G., 2014. FEFLOW: Finite Element Modeling of Flow, Mass and Heat Transport in Porous and Fractured Media. Springer, 2014. ISBN 9783642387395.

Doherty J.E., Hunt R.J., 2010. Approaches to highly parameterized inversion-a guide to using pest for groundwater-model calibration. Scientific Investigations Report 2010-5169. 10.3133/sir20105169.

Edenhofer, O., Carraro, C., Hourcade, J.C., 2012. On the economics of decarbonization in an imperfect world. Clim. Change 114, 1–8. https://doi.org/10.1007/s10584-012-0549-7.

Eppelbaum, L., Kutasov, I., Pilchin, A., 2014. Applied geothermics. Lecture Notes in Earth System Sciences. Springer, Berlin, Germany. https://doi.org/10.1007/978-3-642-34023-9. ISBN 978-3-642-34022-2.

Epting, J., Huggenberger, P., 2013. Unraveling the heat island effect observed in urban groundwater bodies - definition of a potential natural state. J. Hydrol. 501, 193–204. https://doi.org/10.1016/j.jhydrol.2013.08.002.

Epting, J., Handel, F., Huggenberger, P., 2013. Thermal management of an unconsolidated shallow urban groundwater body. Hydrol. Earth Syst. Sci. 17, 1851–1869. https://doi.org/10.5194/hess-17-1851-2013.

Epting, J., Baralis, M., Künze, R., Mueller, M.H., Insana, A., Barla, M., Huggenberger, P., 2020. Geothermal potential of tunnel infrastructures – Development of tools at the City-scale of Basel, Switzerland. Geothermics 83, 101734.

Ferguson, G., Woodbury, A.D., 2006. Observed thermal pollution and post-development simulations of low-temperature geothermal systems in Winnipeg, Canada. Hydrogeol. J. 14, 1206–1215. https://doi.org/10.1007/s10040-006-0047-y.

Fry, V.A., 2009. Lessons from London: regulation of open-loop ground source heat pumps in central London. Q. J. Eng. Geol. Hydrogeol. 42, 325–334. https://doi.org/10.1144/1470-9236/08-087.

García-Gil A., Goetzl G., Maciej R.K., Boon D.P., Abesser C., Janza M., Herms I., Petitclerc E., Erlstr M., Holecek J., Hunter T., Vandeweijer V.P., Cernak R., Mejías M., Epting J., 2020. Governance of shallow geothermal energy resources 138. 10.1016/j.enpol.2020.111283.

Gaur, A.S., Fitiwi, D.Z., Curtis, J., 2021. Heat pumps and our low-carbon future: a comprehensive review. Energy Res. Soc. Sci. 71, 101764. https://doi.org/10.1016/j.erss.2020.101764.

Herbert, A., Arthur, S., Chillingworth, G., 2013. Thermal modelling of large scale exploitation of ground source energy in urban aquifers as a resource management tool. Appl. Energy 109, 94–103. https://doi.org/10.1016/j.apenergy.2013.03.005.

Insana, A., Barla, M., 2020. Experimental and numerical investigations on the energy performance of a thermo-active tunnel. Renew. Energy 152, 781–792. https://doi.org/10.1016/j.renene.2020.01.086.

Insana, A., Barla, M., Aiassa, S., Antolini, F., 2023. Thermal performance of a metro station in Turin equipped with energy geostructures. Expanding Underground - Knowledge and Passion to Make a Positive Impact on the World – Anagnostou, Benardos & Marinos (1st Edition). Proceedings of the ITA-AITES World Tunnel Congress, WTC 2023. CRC Press. ISBN 978-1-003-34803-0.

Insana, A., 2020. Thermal and Structural Performance of Energy Tunnels. PhD Thesis, Politecnico di Torino, Turin.

Junghans, L., 2015. Evaluation of the economic and environmental feasibility of heat pump systems in residential buildings, with varying qualities of the building envelope. Renew. Energy 76, 699–705. https://doi.org/10.1016/j.renene.2014.11.037.

Laloui, L., Di Donna, A., 2013. Energy Geostructures: Innovation in Underground Engineering. ISTE Ltd and. John Wiley & Sons Inc, London, UK.

Lo Russo, S., Gnavi, L., Roccia, E., Taddia, G., Verda, V., 2014. Geothermics Groundwater Heat Pump (GWHP) system modeling and Thermal Affected Zone (TAZ) prediction reliability: influence of temporal variations in flow discharge and injection temperature. Geothermics 51, 103–112. https://doi.org/10.1016/j.geothermics.2013.10.008.

Lund, J.W., Boyd, T.L., 2016. Direct utilization of geothermal energy 2015 worldwide review. Geothermics 60, 66–93. https://doi.org/10.1016/j.geothermics.2015.11.004.

Ministero dello Sviluppo Economico, 2015. Decreto interministeriale del 26 giugno 2015: applicazione delle metodologie di calcolo delle prestazioni energetiche e definizione delle prescrizioni e dei requisiti minimi degli edifici. Gazzetta Ufficiale della Repubblica Italiana, Serie generale 162 (in italian). Italy.

Mock, J.E., Tester, J.W., Wright, P.M., 1997. Geothermal energy from the earth: its potential impact as an environmentally sustainable resource. Annu. Rev. Energy Environ. 22, 305–356. https://doi.org/10.1146/annurev.energy.22.1.305.

Perego, R., Dalla Santa, G., Galgaro, A., Pera, S., 2022. Intensive thermal exploitation from closed and open shallow geothermal systems at Urban scale: unmanaged conflicts and potential synergies. Geothermics 103, 102417. https://doi.org/10.1016/j.geothermics.2022.102417.

Quattrocchi, F., Boschi, E., Spena, A., Buttinelli, M., Cantucci, B., Procesi, M., 2013. Synergic and conflicting issues in planning underground use to produce energy in densely populated countries, as Italy. Geological storage of CO2, natural gas, geothermics and nuclear waste disposal. Appl. Energy 101, 393–412. https://doi.org/10.1016/j.apenergy.2012.04.028.

Regione Piemonte, 2007. D.C.R. 117-10731 del 13 marzo 2007. PTA 2007 - Water protection plan (in italian). Italy. https://www.regione.piemonte.it/web/temi/ambiente-territorio/ambiente/acqua/piano-tutela-delle-acque-pta-2007 (accessed 05 November 2023).

Saner, D., Juraske, R., Kübert, M., Blum, P., Hellweg, S., Bayer, P., 2010. Is it only CO2 that matters? A life cycle perspective on shallow geothermal systems. Renew. Sustain. Energy Rev. 14, 1798–1813. https://doi.org/10.1016/j.rser.2010.04.002.

Sethi, R., Di Molfetta, A., 2007. Heat transport modeling in an aquifer downgradient a municipal solid waste landfill in Italy. Am. J. Environ. Sci. 3 (3), 106–110. https://doi.10.3844/ajessp.2007.106.110.

Shewchuk, J.R., 1996. Applied computational geometry towards geometric engineering. In: Lin, M.C., Manocha, D. (Eds.), WACG 1996: Applied Computational Geometry Towards Geometric Engineering, Volume 1148 of Lecture Notes in Computer Science. Springer Berlin Heidelberg, Berlin Heidelberg, pp. 203–222.

Tinti, F., Barbaresi, A., Benni, S., Torreggiani, D., Bruno, R., Tassinari, P., 2015. Experimental analysis of thermal interaction between wine cellar and underground. Energy Build. 104, 275–286. https://doi.org/10.1016/j.enbuild.2015.07.025.

VDI, 2010. VDI-standard. VDI 4640 blatt 1. Therm. Use Undergr.

Vienken, T., Schelenz, S., Rink, K., Dietrich, P., 2015. Sustainable intensive thermal use of the shallow subsurface-a critical view on the status quo. Groundwater 53, 356–361. https://doi.org/10.1111/gwat.12206.